Carbohydrate Polymers **21** (1993) 83–89

Evidence of the presence of large aggregates contaminating amylose solutions

Philippe Roger & Paul Colonna

Institut National de la Recherche Agronomique, rue de la Géraudière, PB 527, 44026 Nantes Cedex 03, France

A rapid and original macromolecular characterisation of amyloses from different origins was conducted using a combination of size exclusion chromatography (SEC) and multi-angle laser light scattering (MALLS) with 0·1 M KOH as solvent. Amylose mean-average light scattering data were too high in comparison with values obtained by intrinsic viscosity and reducing end group analysis. Dependence of polymer dimension on molecular weight ($R \sim M^{\nu}$) was determined for amyloses as well as for two series of pullulan and dextran standards. For pullulans, dextrans and Avebe amylose, the value of the characteristic exponent ν was in good agreement with published results and models for linear and branched polymers in good solvents. For all other amyloses studied, two values of ν were observed, with the first indicating a low dependence of the size on the mass ($\nu \approx 0{\cdot}1$–$0{\cdot}6$) and the second showing a sharp increase ($\nu \approx 0{\cdot}8$–$1{\cdot}4$) at higher molecular weight ($M > 2 \times 10^6$ g/mol). This phenomenon can be explained by the presence of large aggregates eluted at low elution volume.

INTRODUCTION

Amylose, an α-(1,4)-D-glucan, mainly linear, is the second major component of starch (most starches contain *c.* 18–28% amylose). Nevertheless amylose determines some of the main functional properties of starch. These properties are strongly dependent on the macromolecular features of amylose. A minimal molecular weight (MW) of 40 500 g/mol is necessary for amylose gelation (Gidley & Bulpin, 1989). It is therefore of primary importance to possess a technique which characterises rapidly amylose molecular weight.

Among the techniques already used for amylose characterisation, some give only mean-average values, such as classical static light scattering (Banks & Greenwood, 1975; Kodama *et al.*, 1978; Ring *et al.*, 1985), intrinsic viscosity measurement of reducing end group analysis. For a polydisperse polymer, these average values are sometimes not enough to fully predict its functional properties and a technique giving the macromolecular distribution should be more powerful.

High-performance size-exclusion chromatography (HPSEC) alone allows the determination of amylose or amylopectin molecular-weight distribution (MWD) by using pullulan or dextran calibration (Kobayashi *et al.*, 1985; Kennedy & Rivera, 1992). This determination is relative, the molecular structure of the standards used has to be close to the polymer studied, with MW in the same range. Combination of HPSEC with a laser light scattering detector has been widely used in the last few years, especially with low-angle laser light scattering photometers. Hizukuri and Takagi (1984), and Yu and Rollings (1987), determined amylose average MW and MWD in this way.

A key factor in this type of experiment is the choice of the solvent; 0·1 M KOH was chosen, as alkaline solvents had already been used in amylose or amylopectin characterisation by HPSEC (Yu & Rollings, 1987; Suortti & Pessa, 1991). Furthermore, 0·1 M potassium hydroxide has been shown to be a good solvent with synthetic monodisperse amylose fractions (Roger & Colonna, 1992). Finally, the use of this rather aggressive solvent was allowed by the chemical stability of the macroporous phase used in HPSEC.

This paper describes the coupling of an HPSEC

*To whom correspondence should be addressed.

Carbohydrate Polymers 0144-8617/93/$06.00

system with multi-angle laser light scattering (MALLS) for MWD determination of amylose. Relations between size (radius of gyration) and mass were also studied.

EXPERIMENTAL

Materials

Laboratory amylose was isolated from starches of cassava, potato, wheat, normal maize and smooth-seeded peas by the thymol and *n*-butanol complexation method (Banks & Greenwood, 1967). Absence of contamination by amylopectin was assessed by (i) the iodine binding capacity and wavelength at the maximum absorption (λ_{max}) of the blue iodine–amylose complex, (ii) low pressure chromatography on Fractogel® TSK HW-75 (F) from Merck (Darmstadt, Germany). Further purifications were carried out for cereal amyloses (wheat and maize), as previously described by Takeda *et al.* (1986): just after *n*-butanol was removed by heating, aqueous dispersions of amylose were ultracentrifuged (Beckman model XL70, Pala Alto, CA) at 100 000*g* during 1 h, with a rotor (Ti-70) prewarmed at 40°C.

Leached amylose fractions were obtained by successive aqueous leaching (Schoch, 1945) of corn starch in the temperature range 65–95°C by steps of 5°C. Industrial amylose was kindly provided by Avebe GA (Veendam, The Netherlands).

Pullulan P50 was used to calibrate the photodiodes of the light scattering detector. Pullulan, which is a poly α-(1,6)-maltotriose (Showa Denko K.K., Tokyo, Japan) and dextran, which is a poly α-(1,6)-D-glucose (Pharmacia Chemical Co., Piscataway, NJ and Sigma Chemical Co., St Louis, MO) standards were used to verify that light scattering results were consistent with suppliers' values.

Sample preparation

Amylose powders were dispersed in 1 M KOH, gently stirred overnight at 4°C, passed on a sintered filter G4 and then diluted to 0·1 M KOH.

Analytical methods

Intrinsic viscosities ([η], g/ml) were obtained at 25°C in 0·1 M KOH using an automatic Ubbelholde viscometer (Amtec, France) and were calculated using a double extrapolation to zero concentration based on the Huggins and Kraemer equations (Van Krevelen, 1990). A viscosity average MW ($\overline{M}_{v(V)}$) is calculated from intrinsic viscosities according to a Mark–Houwink–Sakurada relation obtained in 0·15 M KOH by Banks and Greenwood (1975):

$$[\eta] = 8{\cdot}36 \times 10^{-3} \overline{M}_{v(V)}^{0{\cdot}77} \quad (1)$$

The number-average MW ($\overline{M}_{n(N)}$) was determined by the modified Park–Johnson method (Hizukuri *et al.*, 1981).

Amylose average values, MW and size distributions were obtained at 25°C by coupling on-line HPSEC, a multi-angle laser light scattering (MALLS) photometer and a refractometer.

The HPSEC system consisted of a Waters 6000 A solvent delivery system, a Valco C6W injector with a 100 μl injection loop, an Erma ERC-3312 degasser (Erma Optical Works Ltd, Japan), a pulse dampener (Touzart and Matignon, France), an Erma ERC-7510 differential refractive index detector (RI), and three Shodex OHpak KB-800 series (300 mm × 8 mm) columns (Showa Denko K.K., Tokyo, Japan). The column packing is a strong poly(hydroxymethylmethacrylate) gel designed for the separation of polysaccharides. They were connected in the order KB-806, KB-805 and KB-804 with an estimated exclusion limit using poly(ethyleneglycol) of 2×10^7, 4×10^6 and 4×10^5 g/mol respectively. The water used was taken from a Milli-RO-6-plus and Milli-Q-plus water purification system (Millipore, Bedford, MA) and the eluent was 0·1 M KOH carefully degassed and filtered through Durapore GV (0·22 μm) membranes from Millipore before use. The mobile phase has a flow-rate of 1 ml/min and was filtered on-line before the injector through Durapore VV (0·1 μm).

The MALLS detector, a Dawn-F fitted with a K5 flow cells and a He–Ne laser (λ = 632·8 nm), from Wyatt Technology Corporation (Santa Barbara, CA), was installed on-line between the columns and the refractometer. Number-average MW ($\overline{M}_n$), weight-average MW ($\overline{M}_w$), *z*-average MW ($\overline{M}_z$), MWD, polydispersity, and root-mean-square (rms) radii in nm ($\overline{R}_G = \langle \overline{r}_g^2 \rangle_z^{1/2}$) were established with ASTRA software (v. 2·02) (Wyatt, 1992). A value of 0·146 ml/g was employed as refractive index increment (d*n*/d*c*) for amylose (Paschall & Foster, 1952).

Prior to injection, all samples were made dust-free by filtering through Durapore HV (0·45 μm) without effects on amylose concentrations which were in the range 0·5–5 g/litre. Concentrations were checked by the sulphuric acid–orcinol colorimetric method (Tollier & Robin, 1979), amylose sample recovery being always greater than 95%.

RESULTS AND DISCUSSION

Light scattering treatment

For each sampling time of the elution pattern corresponding to one elution volume (V_i), a concentration (c_i) is calculated from the differential refractive index

response. Following this determination, the measurement of the light scattered using the 15 Dawn-F photodiodes allows molecular weight (M_i) and radius of gyration ($R_i = \langle r_g^2 \rangle_i^{1/2}$) to be calculated according to the Zimm extrapolation of the light scattered to zero angle degree:

$$\left(\frac{Kc}{\Delta R_\theta}\right)_i = \frac{1}{M_i}\left(1 + \frac{16\pi^2}{3\lambda^2}\langle r_g^2\rangle_i \sin^2(\theta/2)\right)$$

M_i and R_i are obtained respectively from the y-intercept to zero angle and from the slope of the expected straight line. MWD can then be plotted on a curve of c_i (or cumulative c_i) versus M_i.

Average MW values are then calculated according to:

$$\overline{M}_n = \frac{\Sigma_i c_i}{\Sigma_i (c_i/M_i)}$$

$$\overline{M}_w = \frac{\Sigma_i c_i M_i}{\Sigma_i c_i}$$

$$\overline{M}_z = \frac{\Sigma_i c_i M_i^2}{\Sigma_i c_i M_i}$$

$$\overline{M}_v = \left(\frac{\Sigma_i c_i M_i^a}{\Sigma_i c_i}\right)^{1/a}$$

where a is a Mark-Houwink-Sakurada coefficient.

The polydispersity index is the ratio $\overline{M}_w/\overline{M}_n$ and the root-mean-square z-average radius of gyration $\overline{R}_G$ is given by

$$\overline{R}_G^2 = \langle \overline{r}_g^2 \rangle_z = \frac{\Sigma_i c_i M_i \langle r_g^2 \rangle_i}{\Sigma_i c_i M_i}$$

Standards characterisation

Pullulan and dextran commercial standards were used to assess validity of the HPSEC-MALLS experiments. Corresponding values of $\overline{M}_w$ and $\overline{R}_G$ are summarised in Table 1.

A semi-logarithmic plot of $\overline{M}_w$ versus elution volume at the maximum of the RI peak for pullulan and dextran standards is shown in Fig. 1. As expected, for the same elution volume (i.e. hydrodynamic size), the branched polymer exhibits a higher MW than the linear one, due to a higher density or compactness. The regression coefficient of the relation between log $\overline{M}_w$ and elution time was 0·995 for pullulans and 0·991 for dextrans.

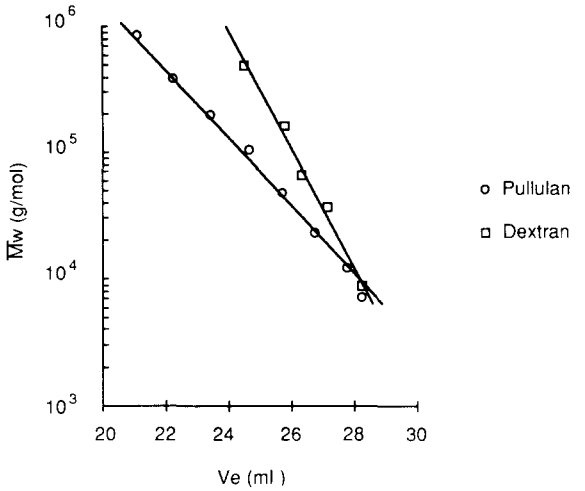

Fig. 1. $\overline{M}_w$ versus elution volume for (□) dextran and (○) pullulan standards.

The MWD or the cumulative MWD can be obtained by this coupling (Fig. 2). However, the greatest interest of the MALLS detector is in providing the relation between size and mass. The relationship between $\overline{R}_G$ and $\overline{M}_w$ obtained for pullulans P800, P400, P200, P100 and P50 was

$$\overline{R}_G = 4{\cdot}02 \times 10^{-3} \overline{M}_w^{0{\cdot}69} \quad r = 0{\cdot}999$$

For standards below 50 000 g/mol, it was difficult to get a reliable $\overline{R}_G$ value because of the low sensitivity of the measuring system, which was restricted by the dimensions of the molecules being too small compared to the wavelength of the laser (Table 1). This restriction still exists for one high MW sample.

For P800, 35% in weight of the information is lost and the radius (R_i) is calculated only for M_i over 6×10^5 g/mol:

$$R_i = 2{\cdot}156 \times 10^{-2} M_i^{0{\cdot}56} \quad r = 0{\cdot}999$$

Table 1. $\overline{M}_w$ and $\overline{R}_G$ of pullulan and dextran standards

Pullulan	$\overline{M}_w$ (10^3 g/mol)	$\overline{R}_G$ (nm)	Dextran	$\overline{M}_w$ (10^3 g/mol)	$\overline{R}_G$ (nm)
P800	833	49·1	T500	490	24·4
P400	386	29·9	58C	161	13·1
P200	198	19·1	T70	64	9·6
P100	102	11·6	T40	36	13·3
P50	47	6·8	T10	9	21·7
P20	23	14·3			
P10	12	18·9			
P5	7	31·3			

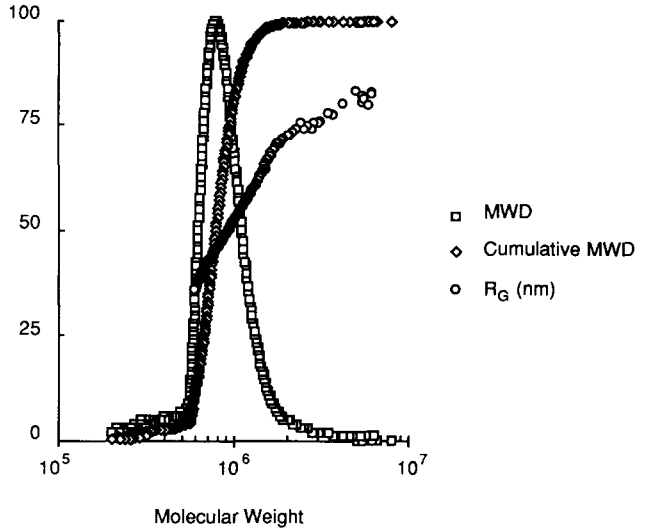

Fig. 2. (□) MWD, (◇) cumulative MWD and (○) radius of gyration versus molecular weight for P800 pullulan standard.

The curvature of the slope observed for the higher MW could be interpreted as evidence of a small degree of branching (Fig. 2).

For T500 dextran, determination of gyration radii begins at $1{\cdot}6 \times 10^5$ g/mol and then dependence of size on mass shows two different behaviours:

$R_i = 3{\cdot}62 \times 10^{-3} M_i^{0{\cdot}65}$ $r = 0{\cdot}992$
for $M_i < 6 \times 10^5$ g/mol

$R_i = 0{\cdot}179 M_i^{0{\cdot}35}$ $r = 0{\cdot}906$
for $M_i > 6 \times 10^5$ g/mol

These observations can be interpreted as follows. Fractions of T500 dextran are linear below 6×10^5 g/mol and slightly branched over 6×10^5 g/mol. Dextrans show a varying degree of branching: this degree of branching increases with increasing molar mass (Fishman *et al.*, 1987), in agreement with the sample studied here.

Amylose sample characterisation

No amylopectin contamination occurs for tubers, potato and cassava amyloses according to values recorded for λ_{max} and limiting binding capacity (Table 2). Corresponding elution profiles on HW75 were free of amylopectin (Fig. 3). Further purifications were carried out for cereal amyloses (wheat and maize). In this way, ultracentrifugation was used, enabling acceptable values for λ_{max} and iodine binding capacity values (Table 2).

HPSEC-MALLS experiments were conducted on all purified laboratory amyloses and an industrial amylose. Both refractometer and light scattering at 90° chromatograms are shown in Fig. 4 for purified potato amylose.

Table 2. Iodine binding capacity and λ_{max} of laboratory and industrial amyloses

Amylose	Iodine binding capacity (mg/100 mg amylose)	λ_{max} (nm)
Laboratory: Cassava	21·6	662
Potato	21·1	655
Wheat	21·7	658
Maize	19·5	650
Pea	20·4	657
Industrial: Avebe	22·0	652

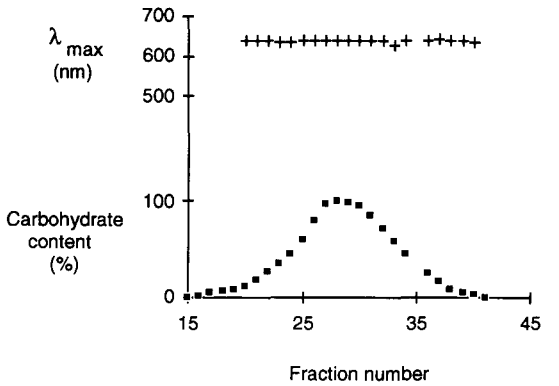

Fig. 3. Cassava amylose elution profile on HW75 with the wavelength at the maximum of absorption (λ_{max}).

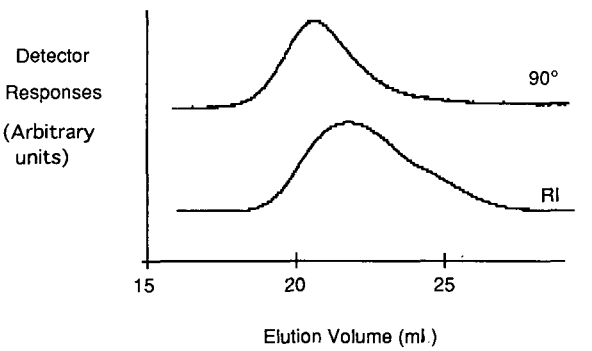

Fig. 4. Refractometer (RI) and light scattering at 90° responses for potato amylose.

Considering laboratory amylose RI elution profiles, cassava amylose is eluted first (V_e = 20·6 ml), reflecting a higher hydrodynamic size, whereas maize amylose is eluted last (V_e = 23 ml). Wheat, potato and pea amyloses are eluted in the order listed (respectively 22, 22·2 and 22·6 ml).

Light scattering results are given in Table 3. Classical macromolecular characteristics are also listed in Table 3: $\overline{M}_{n(N)}$, and $\overline{M}_{v(V)}$ using eqn (1).

Chromatographic results (elution volumes) are in the same rank as intrinsic viscosity values (Table 3) which are also a measurement of the hydrodynamic volume. For laboratory amylose, $\overline{M}_w$ values were between

Table 3. Macromolecular features of amyloses

Amylose	$\overline{M}_n$	$\overline{M}_w$	$\overline{M}_z$	$\overline{M}_v$	$\overline{R}_G$	P	$[\eta]$	$\overline{M}_{v(V)}$	$\overline{M}_{n(N)}$
Cassava	710	1 200	1 600	1 200	77·4	1·7	367	1 100	760
Potato	440	980	1 600	910	71·6	2·2	261	690	400
Wheat	430	1 100	2 600	1 000	80·0	2·6	278	750	275
Pea	300	780	1 900	710	73·0	2·6	253	660	250
Maize	200	870	2 000	760	66·5	4·4	225	570	150
Avebe	140	400	1 300	360	37·7	2·8	150	330	90

All average MW are given in 10^3 g/mol.
P is the polydispersity index: $P = \overline{M}_w/\overline{M}_n$.
$\overline{M}_{v(V)}$ is calculated from the limiting viscosity number $[\eta]$.
$\overline{M}_{n(N)}$ is determined by reducing end group analysis.

$1{\cdot}2 \times 10^6$ g/mol (for cassava) and $7{\cdot}8 \times 10^5$ g/mol (for pea). These values are higher than the results previously published, particularly for maize amylose by Takeda *et al.* (1988): $\overline{M}_w$ of 4×10^5 g/mol. Average MW values determined by other methods (reducing end group analysis and intrinsic viscosity measurement) always lead to higher values than LS average MW. $\overline{M}_n/\overline{M}_{n(N)}$ ratios are in the range 1·1–1·6 and $\overline{M}_v/\overline{M}_{v(V)}$ ratios are in the range 1·1–1·3, with one exception: $\overline{M}_n/\overline{M}_{n(N)} = 0{\cdot}9$ for cassava amylose. Radii of gyration, which ranged from 66·5 nm to 80 nm for laboratory amyloses, were not in the same rank as hydrodynamic volumes. Cassava amylose polydispersity was smallest (1·7) and maize amylose polydispersity largest (4·4) (Table 3). Results for industrial amylose ($\overline{M}_w = 4 \times 10^5$ g/mol, $\overline{R}_G = 37{\cdot}7$ nm, $V_e = 23{\cdot}7$ ml, $[\eta] = 147$ ml/g) presented lower values than laboratory amyloses (Table 3), which could explain the following differences in observed behaviour between size and mass.

The dependence of size upon mass for industrial amylose (Fig. 5) corresponds to the behaviour of a rigid rod for lower MW and of a sphere for the higher MW, as has been previously related by Rollings (1992). For natural amylose, this behaviour was not checked. Influence of molecular weight on amylose size was very low at first, with a characteristic exponent between 0·1 and 0·6, and then increased sharply for MW over 2×10^6 g/mol (Fig. 6).

In addition, relationships between size and mass were accessible only for M_i over 8×10^5 g/mol. So it was not possible to observe the possible change of the conformation near the 'dissolving gap' described by Burchard (1963) on monodisperse synthetic amylose, around 2×10^5 g/mol.

An aqueous leaching was attempted to access these low MW dimensions. Seven amylose fractions were obtained by successive aqueous leaching of a corn starch in the temperature range 65–95°C in steps of 5°C. For the lower leaching temperature (65–80°C), refractive index profiles (Fig. 7(a)) present only one

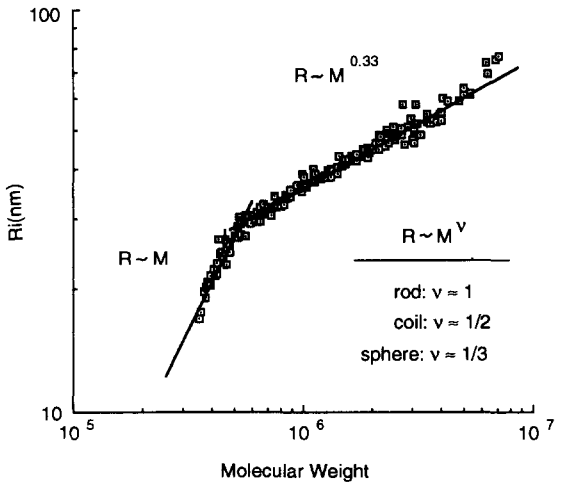

Fig. 5. Radius of gyration (R_i) versus MW obtained for industrial amylose.

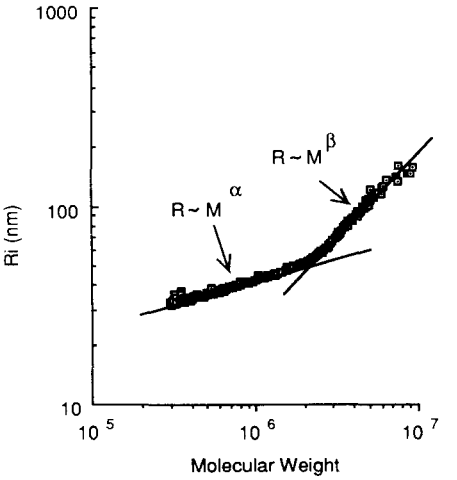

AMY	α	β
Cassava	0.6	1.4
Potato	0.2	0.8
Wheat	0.1	1.3
Pea	0.3	1.1
Maize	0.1	1.3

Fig. 6. Radius of gyration (R_i) versus MW for laboratory amylose obtained by the complexation method.

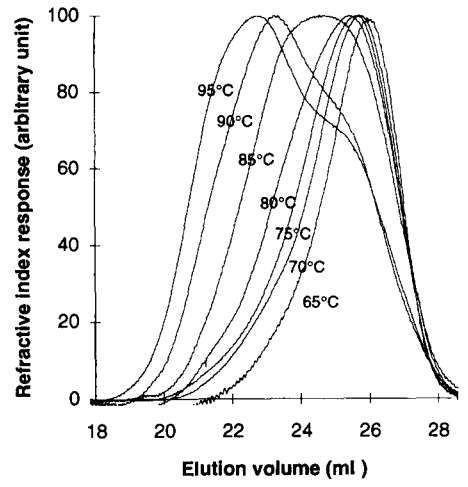

(a)

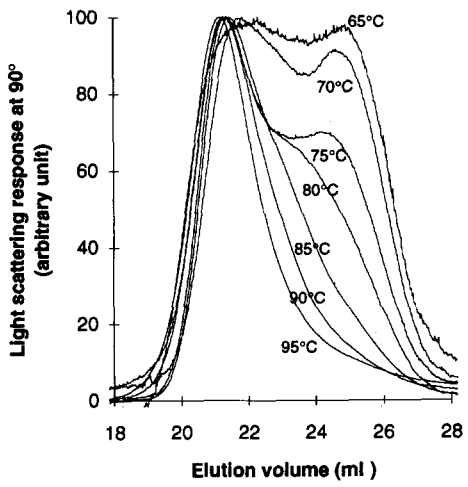

(b)

Fig. 7. (a) Refractometer, and (b) light scattering at 90°, responses of leached corn amylose.

peak (V_e from 26 to 25·5 ml). As the leaching temperature increases, the RI peak becomes broader and shifts to elution volumes of 25, 23 and 22·5 for T = 85, 90 and 95°C respectively. The higher leaching temperatures (90 and 95°C) lead clearly to a distinctive shoulder towards the higher elution volume. This phenomenon is more striking when followed by light scattering profiles (Fig. 7(b)), where even for the lower leaching temperature a peak is eluted at low elution volume (*c.* 21·5–22 ml). The combination of these responses demonstrates the presence of at least two populations in all the samples obtained by leaching.

The discrepancy between the RI and MALLS responses can be explained by the presence of a supermolecular structure of high MW present at a small amount and contaminating all the natural amyloses studied here. This contamination is clearly observable for the lower amylose leaching temperatures where there is a high light scattering peak (Fig. 7(a)) and no corresponding refractive index response (Fig. 7(b)) at low elution volume (*c.* 21·5–22 ml). For higher amylose $\overline{M}_w$ values obtained either by thymol complexation or by high leaching temperature, there is only one tiny light scattering peak, which is due mainly to the light scattered by the superstructure. In any case, this contamination leads to erroneous $\overline{M}_w$ values and explains the high values in Table 3.

Yu and Rollings (1987) studied an amylose of DP ≈ 110 by coupling HPSEC-LALLS and using 0·5 N NaOH as solvent. The LS chromatogram presented in Fig. 2(a) of the corresponding reference indicates clearly an analogue peak at low elution volume. Taking into account all recorded data, they estimated an $\overline{M}_w$ of $2{\cdot}2 \times 10^5$ g/mol by HPSEC-LALLS analysis, leading to a polydispersity index as high as 12.

This contamination prevents any further MWD validation in those conditions and could explain the unusual relation between size and mass obtained for laboratory amyloses. Even the structure obtained for the industrial amylose is doubtful.

At this stage, the composition of this high MW population is questionable. It is now admitted that amylose possesses a fraction of branched molecules (Hizukuri *et al.*, 1981). But it seems unlikely that these branched molecules represent the population eluted individually at low volume in HPSEC-MALLS, as branching causes an increase in elution volume. This peak could be a result of an association between some special amylose chains. Those amylose chains which could form aggregates could be either slightly more branched, or more polyelectrolyte than the majority of the population.

A more reasonable interpretation would be the presence of remaining amylopectin undetectable by the classical physico-chemical characterisation with iodine.

CONCLUSION

The coupling between HPSEC and MALLS provided fruitful information about polysaccharide conformation in solution. On a single polymer, relationships between size and mass are obtained and conformation changes can be studied. Amylose elutes without detectable retention on HPSEC columns, which is not the case for amylopectin. Nevertheless, an aggregation peak is revealed by SEC-LS chromatograms of lab amyloses and is directly observable only for the samples of lower average molecular weight. This association phenomenon is responsible for higher average $\overline{M}_w$ values than those expected and for the anomalous relationship between size and mass. This aggregation process is not fully explained and further investigations are needed.

REFERENCES

Banks, W. & Greenwood, C.T. (1967). *Die Stärke*, **19,** 394–8.

Banks, W. & Greenwood, C.T. (1975). *Starch and its Components*. Edinburgh University Press, Edinburgh.

Burchard, W. (1963). *Macromol. Chem.*, **64,** 110–25.

Fishman, M.L., Damert, W.C., Philipps, J.G. & Barford, R.A. (1987). *Carbohydr. Res.*, **160,** 215–25.

Gidley, M.J. & Bulpin, P.V. (1989). *Macromolecules*, **22,** 341–6.

Hizukuri, S. & Takagi, T. (1984). *Carbohydr. Res.*, **134,** 1–10.

Hizukuri, S., Takeda, Y. & Yasuda, M. (1981). *Carbohydr. Res.*, **94,** 205–13.

Kennedy, J.F. & Rivera, Z.S. (1992). *Starch/Stärke*, **44,** 53–5.

Kobayashi, S., Schwartz, S.J. & Lineback, D.R. (1985). *Chromatogr.*, **319,** 205–14.

Kodama, M., Noda, H. & Kamata, T. (1978). *Biopolymers*, **17,** 985–1002.

Paschall, E.F. & Foster, J.F. (1952). *J. Polym. Sci.*, **9,** 85–92.

Ring, S.G., I'Anson, K.J. & Morris, V.J. (1985). *Macromolecules*, **18,** 182–8.

Roger, P. & Colonna, P. (1992). *Carbohydr. Res.*, **227,** 73–83.

Rollings, J.E. (1992). In *Laser Light Scattering in Biochemistry*, ed. S.E. Harding. The Royal Society of Chemistry, Cambridge, UK, pp. 275–93.

Schoch, T.J. (1945). *Adv. Carbohydr. Chem.*, **1,** 247–75.

Suortti, T. & Pessa, E. (1991) *J. Chromatogr.*, **536,** 251–4.

Takeda, Y., Hizukuri, S. & Juliano, B.O. (1986). *Carbohydr. Res.*, **148,** 299–308.

Takeda, Y., Shitaozono, T. & Hizukuri, S. (1988). *Starch/Stärke*, **40,** 51–4.

Tollier, M.T. & Robin, J.P. (1979). *Ann. Tech. Agric.*, 1–15.

Van Krevelen, D.W. (1990). *Properties of Polymers*. Elsevier, Amsterdam, pp. 243–83.

Wyatt, P.J. (1992). In *Laser Light Scattering in Biochemistry*, ed. S.E. Harding. The Royal Society of Chemistry, Cambridge, UK, pp. 35–58.

Yu, L.P. & Rollings, J.U. (1987). *J. Appl. Polym. Sci.*, **33,** 1909–21.